



STRUCTURAL SCIENCE
CRYSTAL ENGINEERING
MATERIALS

Volume 75 (2019)

Supporting information for article:

**Solvatochromism and Mechanochromism Observed in a Triphenyl-
amine Derivative**

**Chunyang Guo, Qi Zhang, Bingqing Zhu, Bin Zhu, Weiqun Zhou, Guobin Ren
and Xuefeng Mei**

Content

I. Experimental section

II. Synthesis of the intermediates and target molecule

III. Figures and Tables

Figure S1. ¹H NMR spectrum of TPA-CBH.

Figure S2. a and b are normalized UV-vis absorption spectra of TPA-CBH in different polar solvents.

Table S1 Physical properties of TPA-CBH in different polar solvents.

Figure S3 Normalized PL spectra of TPA-CBH in different polar solvents.

Figure S4. Normalized UV-vis absorption spectra of TPA-CBH in THF and THF/water mixtures with different volume fractions of water.

Figure S5 PL spectra of TPA-CBH (5.0×10^{-5} mol L⁻¹) in THF and THF/water mixtures with different volume fractions of water.

Figure S7 PXRD and DSC patterns of TPA-CBH in different phases.

Figure S8. Overlay of four symmetry-independent molecules of two forms by keeping the A ring as the fixed fragment.

Figure S9 FT-IR spectrums of Amorphous (green), Form A (red), and Form B (blue).

Table S2. List of intermolecular hydrogen bond lengths and angles for the two crystalline forms

I. Experimental section

Materials. All the starting materials and solvents employed in this work were commercially available, and can be used without any purification. Triphenylamine, 4-Methoxyphenylamine, POCl₃ were purchased from J&K (CHINA). All analytical grade solvents were purchased from Sinopharm Chemical Reagent Company, Ltd. and used without further purification.

X-ray powder diffraction (XRPD). XRPD patterns were measured at ambient temperature on a Bruker D8 Advance diffractometer using copper radiation (Cu-K α). Data over the range 3-40° 2 θ were collected with a scan speed of 0.10 °·step⁻¹. The voltage and current were 40 kV and 40 mA, respectively. The data were imaged and integrated with RINT Rapid and peak-analyzed with Jade 6.0 from Rigaku.

Single-Crystal X-ray Diffraction (SCXRD). X-ray diffractions of Form A single crystal were performed at 205 K on a Bruker Apex II CCD diffractometer using Mo-K α radiation (λ = 0.71073 Å), and Form B were collected with a Bruker D8 Venture single-crystal diffractometer (Cu K α , λ = 1.54178 Å). The data integration and scaling was processed with SAINT software, and absorption corrections were performed using the SADABS program. The structures were solved by direct method and refined on F2 by the full-matrix least-squares technique using SHELXL-2014 program package. All non-hydrogen atoms were refined with anisotropic displacement parameters. The remaining hydrogen atoms were placed in calculated positions and refined with a riding model. CCDC 1864227 and 1864228 contain the supplementary crystallographic data for this paper. These data are supplied free of charge by The Cambridge Crystallographic Data Centre.

Differential Scanning Calorimetry (DSC). The samples were placed in open aluminum oxide pans and heated at 10 °C·min⁻¹ to 400 °C. DSC experiments were performed on a DSC TA Q2000 instrument under a nitrogen gas flow of 50 mL·min⁻¹ purge. Ground samples weighing 2-3 mg were heated in sealed aluminum pans from 40 to 270 °C with a scan rate of 10 °C·min⁻¹. Two-point calibration using indium and tin was carried out to check the temperature axis and heat flow of the equipment.

¹H-NMR Spectra. The ¹H-NMR spectra were measured on a Varian-MERCURY Plus-400 (400MHz) in deuterated dimethyl sulfoxide (DMSO) using tetramethylsilane (TMS; δ = 0) as internal reference.

Fluorescence spectra. Solid-state fluorescent spectra (SFS) were collected by a Hitachi F-7000 fluorescence spectrophotometer that has a 650-0161 solid sample holder under the scan speed of 240 nm/min with 5 nm emission and excitation slit. The liquid fluorescent spectra were obtained on a CARY50 UV-VIS spectrophotometer and an FLS920 fluorescence spectrophotometer. The relative fluorescence quantum yields were calculated relative to the solutions of 5 × 10⁻⁵ mol L⁻¹ quinine sulfate (ϕ_f = 0.55) in 0.1 mol L⁻¹ sulfuric acid solution as a reference sample, and the absolute solid fluorescence quantum yields were obtained by HORIBA Fluorolog-3 with an integral sphere system.

II. Synthesis of the intermediates and target molecule

Synthesis of N,N-di(4-phenyl)amino] benzaldehyde

Phosphorous oxychloride (POCl₃) (29.5 mL, 316 mmol) was added dropwise into anhydrous N,N-dimethylformamide (DMF) (30 mL, 389 mmol) under 0 °C. After stirred at room temperature for 40min, TPA (2.5 g) was added into the mixture, and the reaction mixture was stirred and heated at 45 °C for 14 hours. After cooling down to room temperature, the reaction mixture was poured into cold water and extracted with chloroform. The combined organic layer was dried with anhydrous MgSO₄, filtered. The combined organic solution was purified by column chromatography, and white compound N,N-di(4-phenyl)amino] benzaldehyde was obtained.

Synthesis of 4-[N,N-di(4-phenyl) amino] benzaldehyde 4-chlorobenzoyl hydrazone

Ethanol (6 mL) and acetic acid (20 μ L) was added into the mixture of N,N-di(4-phenyl)amino] benzaldehyde and 4-chlorobenzoyl hydrazine. The suspension was stirred at 60°C for 6 hours. The product was filtered and washed with ethanol, and recrystallized from ethanol to yield the Compound TPA-CBH as yellow solid.

TPA-CBH [4-[N,N-di(4-phenyl) amino] benzaldehyde 4-chlorobenzoyl hydrazine]: ^1H NMR (400 MHz, DMSO- d_6) δ 11.78 (s, 1H), 8.35 (s, 1H), 7.92 (d, $J = 8.5$ Hz, 2H), 7.64 - 7.55 (m, 4H), 7.35 (t, $J = 7.8$ Hz, 4H), 7.14 - 7.06 (m, 6H), 6.95 (d, $J = 8.5$ Hz, 2H).

III. Figures and Tables

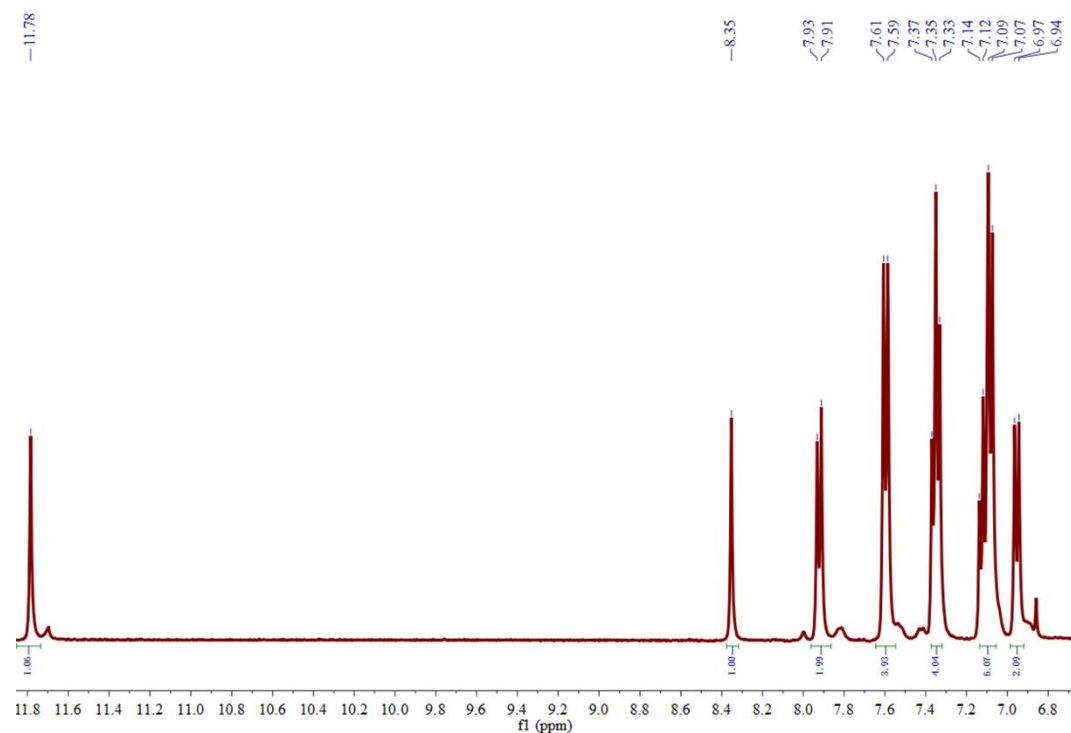


Fig.

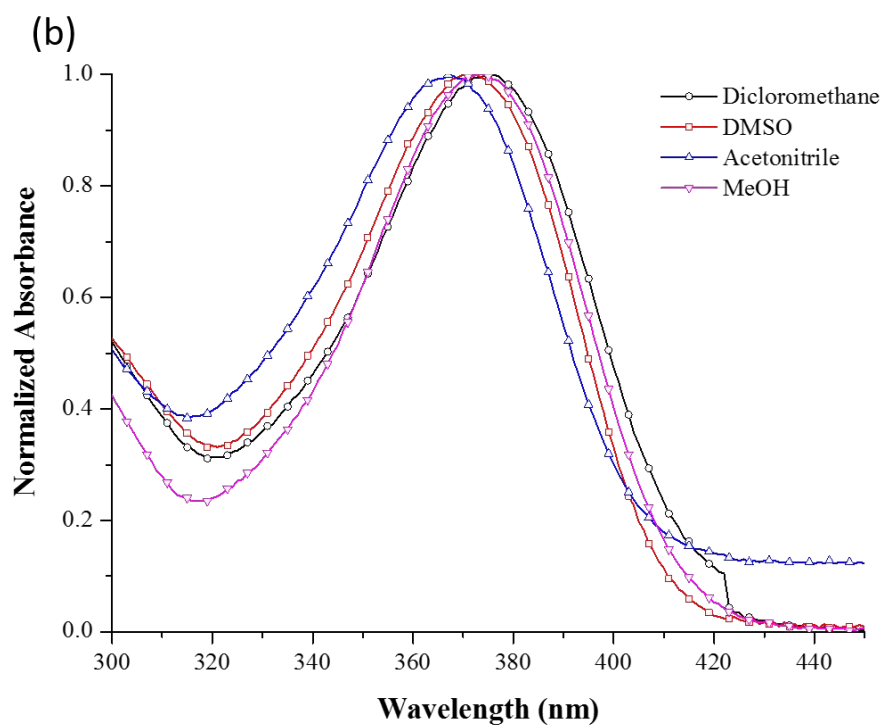
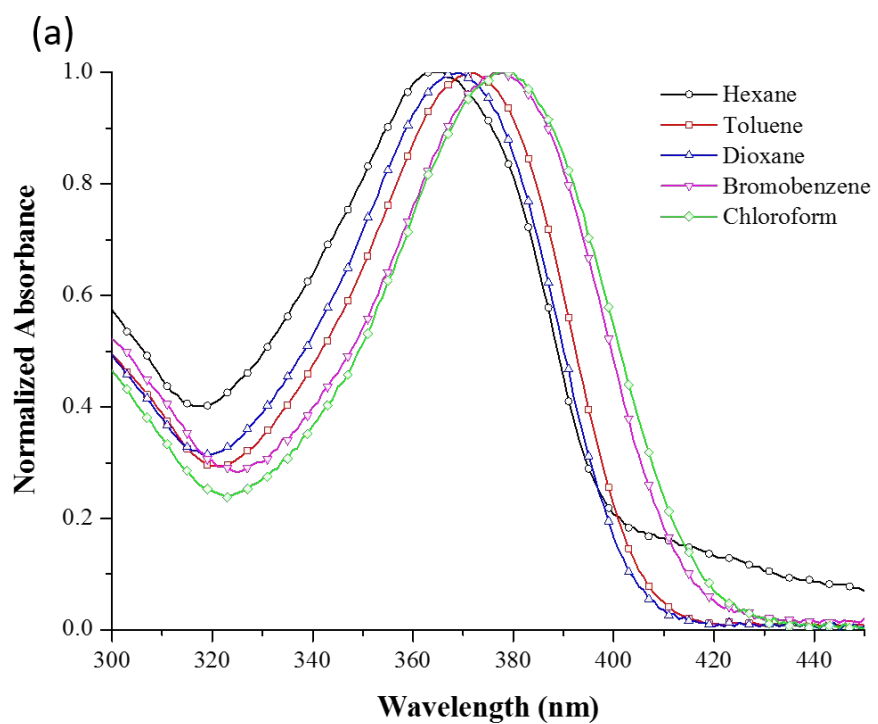


Figure S2. a and b are normalized UV-vis absorption spectra of TPA-CBH in different polar solvents.

Table S1 Physical properties of TPA-CHB in different polar solvents.

Solvents	$f(\epsilon, n)$	$\lambda_{ab}(nm)$	$\lambda_{em}(nm)$	$\Delta\nu(cm^{-1})$
Hexane	0.001225	363	404	2796
Toluene	0.002646	372	430	3626
1,4-dioxane	0.021292	369	433	4006
Bromobenzene	0.12827	378	450	4233
Chloroform	0.149202	379	459	4599
Dichloromethane	0.216582	376	468	5228
DMSO	0.264201	372	474	5785
Acetonitrile	0.305454	367	479	6371
Methanol	0.309339	373	498	6729

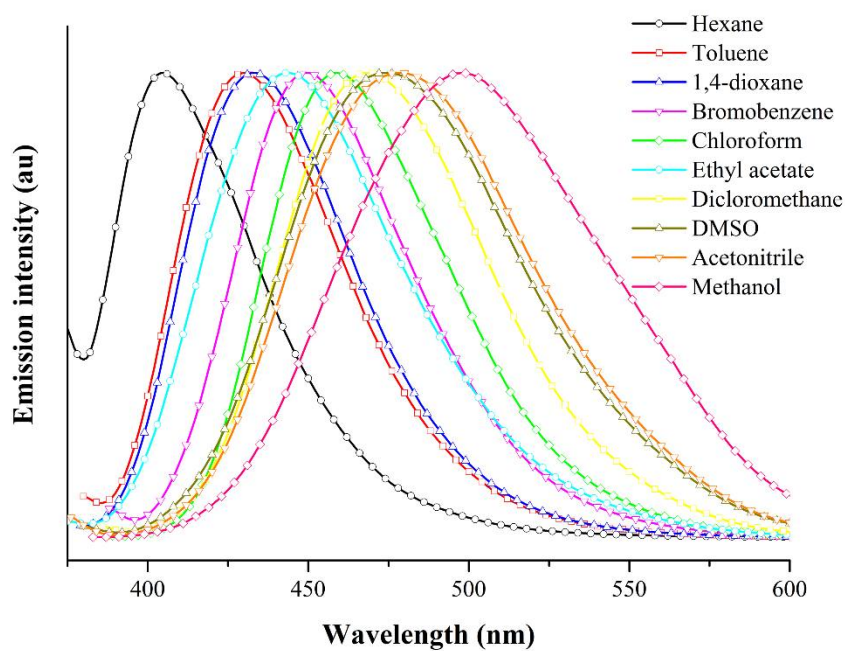


Figure S3 Normalized PL spectra of TPA-CBH in different polar solvents.

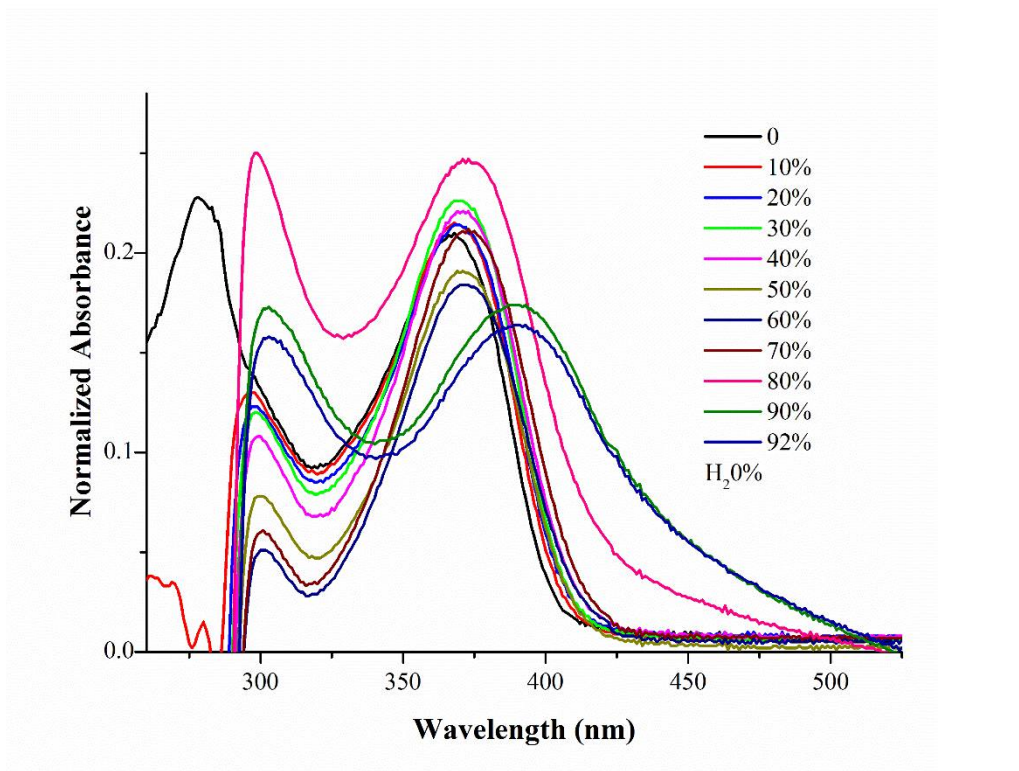


Figure S4. Normalized UV-vis absorption spectra of TPA-CBH in THF and THF/water mixtures with different volume fractions of water.

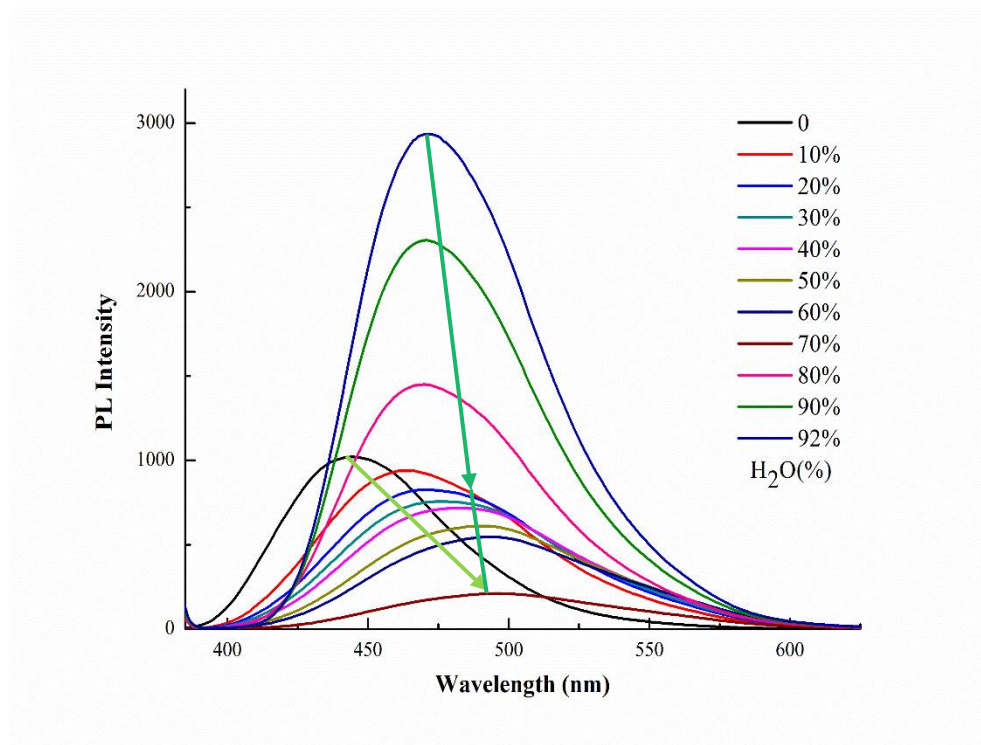


Figure S5 PL spectra of TPA-CBH ($5.0 \times 10^{-5} \text{ mol L}^{-1}$) in THF and THF/water mixtures with different volume fractions of water.

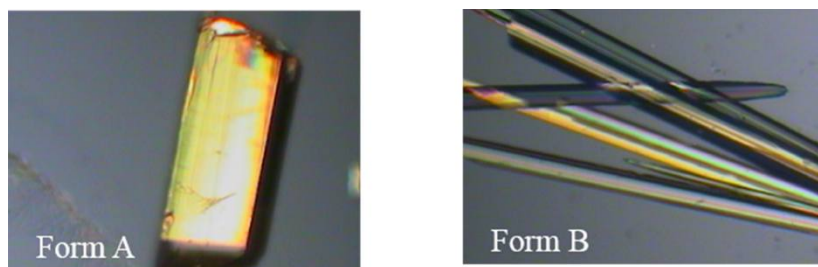


Figure S6 Polarized optical images of Form A and Form B.

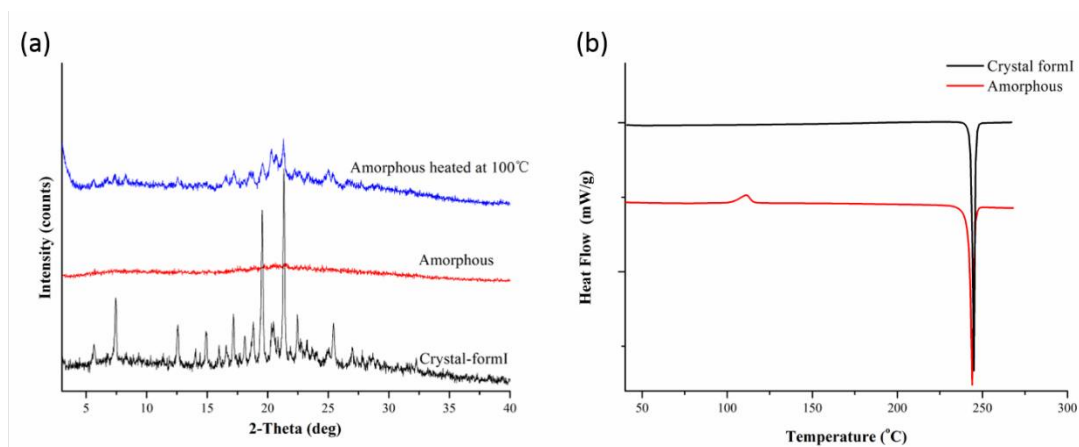


Figure S7 PXRD and DSC patterns of TPA-CBH in different phases.

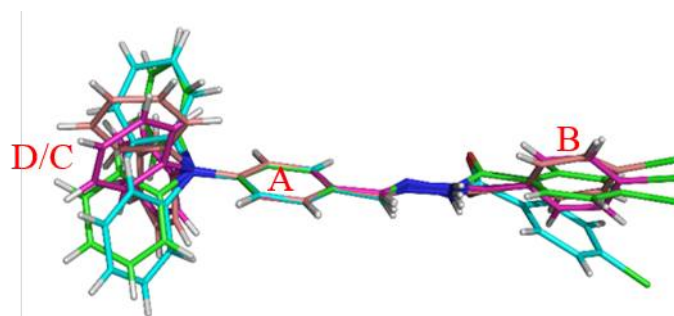


Figure S8. Overlay of four symmetry-independent molecules of two forms by keeping the A ring as the fixed fragment.

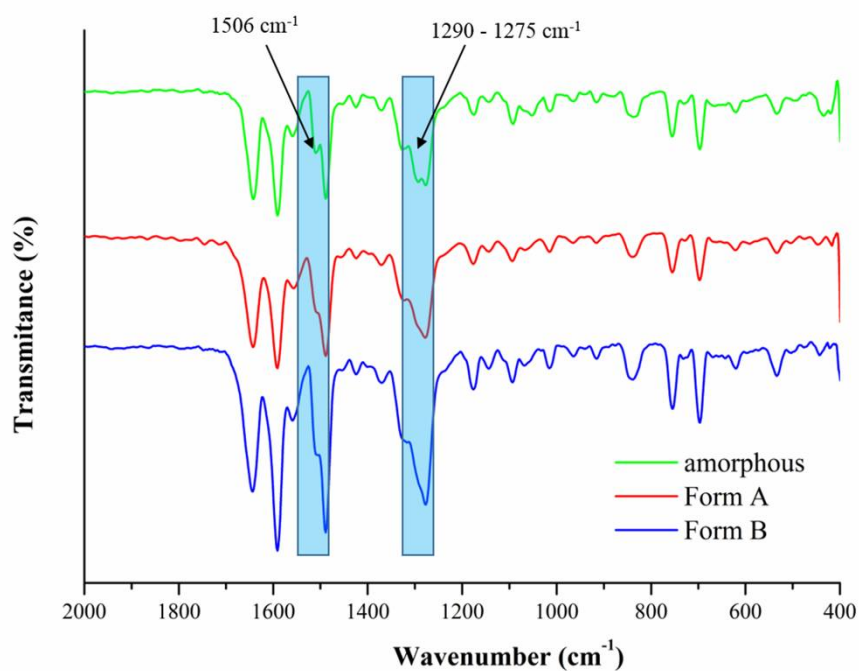


Figure S9 FT-IR spectra of Amorphous (green), Form A (red), and Form B (blue).

Table S2. List of intermolecular hydrogen bond lengths and angles for two crystalline forms

Form	Interactions	H...A/Å	D...A/Å	<D-H...A/°
Form A	N3-H3...O3	2.39	3.192(2)	153
	N6-H6A...O1	2.38	3.181(2)	153
	C22-H22...O2	2.36	3.224(2)	153
Form B	N3-H3...O2	2.11	2.928(3)	154
	N6-H6...O1	2.15	2.894(3)	142
	C2-H2...N5	2.54	3.424(3)	161
	C45-H45...N5	2.54	3.263(3)	133
	C48-H48...O1	2.58	3.272(3)	130
	C52-H52...O2	2.47	2.792(3)	100